Accepted Manuscript

Implementing a two-layer feed-forward catalytic DNA circuit for enzyme-free and colorimetric detection of nucleic acids

Hadi Ravan

PII: S0003-2670(16)30062-9

DOI: 10.1016/j.aca.2016.01.013

Reference: ACA 234353

To appear in: *Analytica Chimica Acta*

Received Date: 10 October 2015

Revised Date: 2 January 2016

Accepted Date: 7 January 2016

Please cite this article as: H. Ravan, Implementing a two-layer feed-forward catalytic DNA circuit for enzyme-free and colorimetric detection of nucleic acids, *Analytica Chimica Acta* (2016), doi: 10.1016/j.aca.2016.01.013.

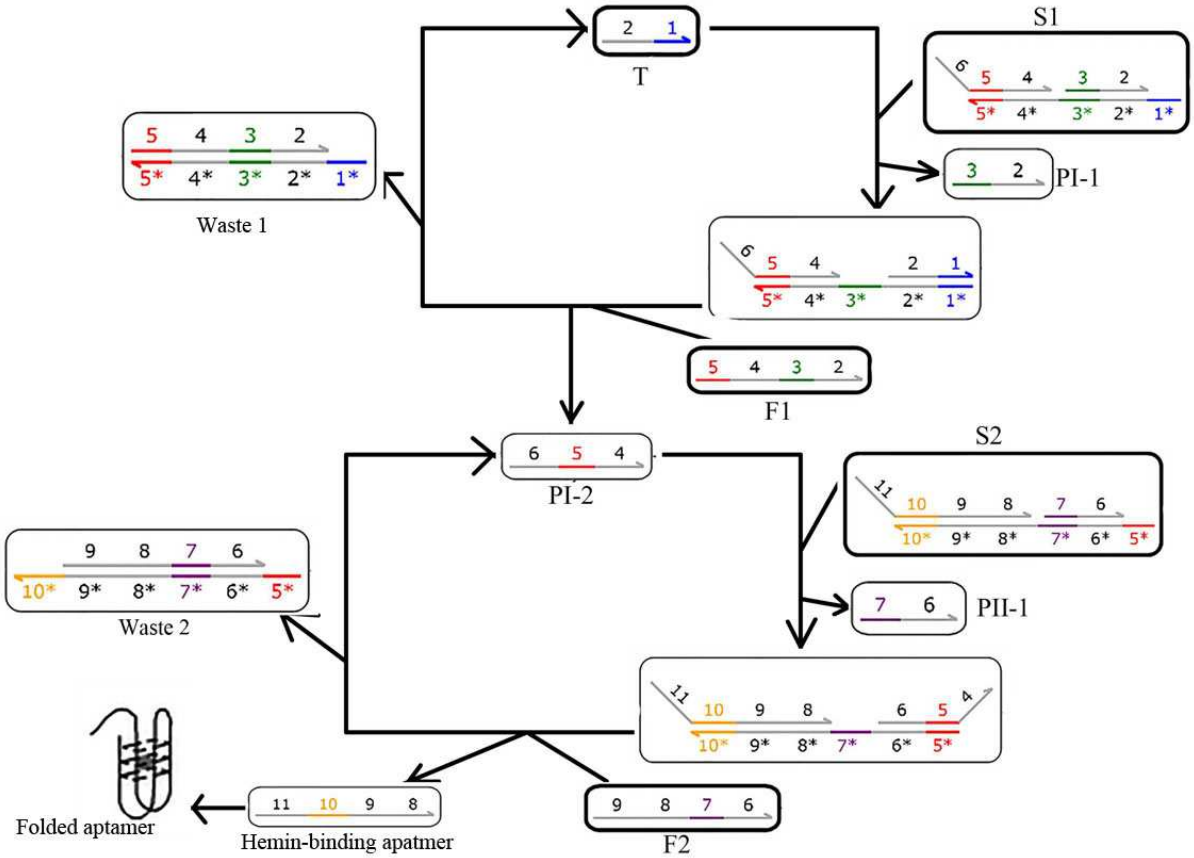

Implementing a two-layer feed-forward catalytic DNA circuit for enzyme-free and colorimetric detection of nucleic acids

Hadi Ravan

Department of Biology, Faculty of Science, Shahid Bahonar University of Kerman, Kerman, Iran

Corresponding Author

Dr. Hadi Ravan

Department of Biology, Faculty of Science, Shahid Bahonar University of Kerman, 76169-14111 Kerman, Iran

Fax: +98 34 33222032, E-mail: ravan@uk.ac.ir

Abstract

In the present study, a highly sensitive and specific bio-sensing platform for enzyme-free and colorimetric detection of nucleic acids was developed. The biosensor is composed of two DNA nanostructures and two fuel strands that construct the foundation of a feed-forward catalytic DNA circuit. Upon binding the target strand to a specific DNA nanostructure, the circuit is run in order that at the end a hemin-binding aptamer, with the ability to convert a colorless substrate into a colored substance is released. Based on this strategy, 4 pM of the target DNA can be easily detected in serum samples by naked eyes after only a two-hour incubation with the circuit; meanwhile, if the incubation time is extended to three hours, the biosensor can detect 1 pM of the target DNA. Besides the elevated sensitivity, the circuit can truly discriminate a spurious target containing one nucleotide mismatch with high specificity. Overall, the enzyme-free catalytic DNA circuit could be used as a sensitive alternative method to enzyme-based biosensors for the specific and cost-effective detection of nucleic acids.

Keywords: Colorimetric Detection, Nucleic Acids, HRP-mimicking DNAzyme, Feed-forward Catalytic DNA Circuit, DNA Circuit, Toehold Exchange

1- Introduction

One of the main aspects of living cells is their ability to transduce and amplify a low extracellular signal to a huge intracellular response. The discovery of such phenomena in living organisms has inspired researchers to develop signal amplifiers that are able to detect a low concentration of an input biomolecule for producing a high signal output. In this respect, several signal amplification strategies have been exploited for bio-sensing of nucleic acids, including enzyme-mediated signal amplification [1-3], nanoparticle-based signal enhancement [4, 5], DNA template reactions [6], and enzyme-free nucleic acid circuits [7, 8]. Among them, enzyme-free DNA circuits due to robustness across diverse conditions [9, 10], low cost in terms of dependency to sophisticated reagents such as protein enzymes, and programmability of the reaction networks [11, 12] have recently become more popular.

Non-enzymatic nucleic acid circuits can be divided based on the reaction strategy into three major classes, including entropy-driven catalysis (EDC), hybridization chain reaction (HCR), and catalytic hairpin assembly (CHA) [13]. The functional part of all classes is a single-stranded toehold domain containing between 3 and 8 nucleotides that binds to an input nucleic acid [14-16]. Upon binding of the toehold, a reversible strand displacement reaction occurs between the target and one or more pre-hybridized strands. However, these amplifiers in the basic format have not been sensitive enough to be used in diagnostic applications. To further improve signal amplification, in the present study, an amplification strategy by combining a two-layer catalytic

DNA circuit with an HRP-mimicking DNAzyme sequence was developed. The assay provides a highly sensitive, highly specific, enzyme-free and colorimetric detecting platform for nucleic acids.

Figure 1 represents the analytical framework of the feed-forward catalytic DNA circuit for the detection of nucleic acids. The circuit is composed of two substrate nanostructures, S1 and S2 and two fuel strands, F1 and F2 (each DNA sequence contains several functional domains labeled numerically) (Table S1). The reaction is initiated by hybridization of a target strand T to the toehold domain 1* on the S1 complex. After binding, a strand displacement reaction can occur between domain 2 of the T strand and a pre-hybridized strand, PI-1, on S1 complex. Then, domain 3 of the PI-1 spontaneously dissociates and provides a binding site for domain 3 of the F1 strand. With a new toehold-mediated strand displacement reaction, the other pre-hybridized strand, PI-2, is released and enters the second layer of the circuit. In addition, upon hybridization of the F1 strand, the T strand is also dissociated and enters a new cycle of PI-2 generation. At the second layer, PI-2 acts as the input and triggers the release of a sequestered HRP-mimicking DNAzyme sequence from S2 complex. Here, PI-2 is also released in a manner like the T strand. In this feed-forward circuit (the output of one layer serves as the input for the subsequent layer), a single target can generate many PI-2s and activate many DNAzyme molecules. Based on this strategy, the two-layer DNA circuit can detect a target DNA 150 times more sensitive than the one-layer DNA circuit.

2- Materials and Methods

2-1 Reagents

DNA oligonucleotides designed in this study were synthesized by Bioneer Co. (South Korea), which were purified by the polyacrylamide gel electrophoresis (PAGE) method. Table S1 represents the domain sequences of the circuit. 2, 2′-Azino-bis(3-ethylbenzothiazoline-6-sulfonic acid) (ABTS) and hemin were purchased from Sigma-Aldrich Chemical Co. (USA). The hemin stock solution was prepared in dimethyl sulfoxide (DMSO) and stored in the dark at -20 °C. All other reagents were of analytical grade.

2-2 Colorimetric measurements

To construct substrate nanostructures, each strand participant in the structure was mixed in HEPES (4-(2-hydroxyethyl)-1-piperazineethanesulfonic acid) Buffered Saline (HBS; 10 mM HEPES buffer containing 200 mM NaCl, 20 mM KCl and 1.5 mM $MgCl_2$, pH 7.4). The samples were heated to 95 °C and slowly cooled down to 25 °C at the rate of 1 °C/min. The annealed nanostructures were purified by non-denaturing PAGE based on Qian procedure with some modifications [17]. To obtain better yields in gel purification, the DNA nanostructures were prepared at a high concentration of their components (40 μM of each oligonucleotide). After hybridization, the substrate complexes were loaded on 12% non-denaturing PAGE (19:1 acrylamide: bisacrylamide, 240 μL ammonium persulfate, and 24 μL Tetramethylethylenediamine (TEMED)). The gels were stained with ethidium bromide, and then visualized under UV light. The proper band of the

substrates were cut out and eluted in 2 mL of HBS buffer for 2 days. The purified nanostructures were quantified by measuring the absorbance intensity at 260 nm [17]. A solution containing 300 nM of each substrate nanostructure and 350 nM of each fuel strand were mixed with different concentrations of the target strand T (from 1 pM to 50 nM) for 3 hours at 37 °C. Hemin was added to the solution at the final concentration of 300 nM and incubated for another 30 min. Then, the peroxidase-mimicking reaction was started by the addition of 2 mM H_2O_2 and 2 mM ABTS. The colorimetric result was measured at 414 nm after 10 min incubation, using a BioTek Microtiter plate reader.

2-3 Analysis of the circuit behavior with PAGE

Non-denaturing PAGE was performed on 12% acrylamide (19:1 acrylamide: bisacrylamide) to analyze the substrates and circuit behavior. Non-denaturing loading dye containing 0.04 g Bromophenol Blue in 50% glycerol was added in a ratio of 1:5 (V/V) to the samples. The electrophoresis was run in Tris-acetate EDTA (TAE) buffer (40 mM Tris, 20 mM acetic acid, 1.5 mM $MgCl_2$ and 1 mM EDTA, pH 8.0) at 180 V for 1 hour. The gels were stained with ethidium bromide for 30 min, and then visualized by a gel documentation system.

2-4 The detection of target strand in artificially spiked serum samples

In order to analyze the efficiency of the biosensor in biological samples, several serum samples were harvested and diluted with HBS containing 1 mM EDTA at 1:6 ratio. The diluted samples were artificially spiked with different concentrations of the target strand. To the samples, 300 nM of each substrate

nanostructure and 350 nM of each fuel strand were added and incubated for 3 hours at 37 °C. Then, hemin was added at a final concentration of 300 nM for 30 min. Finally, the reaction was started by the addition of peroxidase substrate (2 mM H_2O_2 and 2 mM ABTS), and the absorbance was measured at 414 nm after 10 min incubation [21].

3- Results and discussion

In the present study, a two-layer catalytic DNA circuit that provides a highly sensitive and specific detecting platform for nucleic acids was developed. The target nucleic acid triggers to run a cascade of DNA strand displacement reactions in a way that at the end a hemin binding aptamer is released. The aptamer folds into a G-quadruplex peroxidase-mimicking DNAzyme, namely PW17 (domains 11—10—9 in Figure 1), that has recently been used for designing various colorimetric and chemiluminescent assays [18-21]. One of the challenges regarding the use of guanine-rich sequences in the design of DNA circuits is the folding of the sequences by unpredictable non-canonical base-pairs [22]. In this respect, I made minimal use of the guanine repeats in the design of the circuit, except for the DNAzyme sequence. For instance, the F2 strand that was similar to a part of the DNAzyme sequence was truncated by removing the domain 10 from its 5′ end. Although this trimming seems to thermodynamically disfavor the circuit function, the strand displacement reactions proceed acceptably well to release the aptamer sequence.

3-1 Analysis of the circuit behavior with PAGE

158 At first, the efficacy of the circuit was analyzed by non-denaturing PAGE. As
159 shown in Figure S1, in the absence of the target strand, almost no reaction
160 between fuels and substrate nanostructures occurred even after a prolong
161 incubation. This means that the substrate nanostructures are stable in the
162 solution medium. Meanwhile, in the presence of the target strand, the
163 substrate nanostructures are consumed and new electrophoretic bands
164 belonging to the hemin-binding aptamer as well as waste products appear.
165 These results indicate that the target strand can properly run the circuit in
166 order to release a large number of the aptamer molecules.

167 *3-2 Optimizing the concentration of the fuel strands*

168 Since the fuel strands provide the running energy of the circuit, the optimum
169 concentration of those components must be determined. In this respect, 300
170 nM of each substrate complex and 0.3 nM of the target strand were mixed with
171 different concentrations of the fuel strands ranging from 300 to 360 nM. The
172 optimum concentration of the fuel strands was determined to be 350 nM and
173 used for other circuit optimizations (Figure S2).

174 It should be noted that in order to obtain the optimal concentration of the
175 substrates, different concentrations of the DNA nanostructures (0 to 500 nM,
176 interval 50 nM, and 1:1 ratio) were incubated with 1 pM target DNA (the LOD
177 value) for 3 hours. The results revealed that the absorption intensity gradually
178 increased as the substrate concentration increases from 50 to 300 nM (data
179 not shown). In concentrations higher than 300 nM, however, absorption

intensity does not experience any changes. This concentration was chosen as the optimal one.

3-3 Optimizing the incubation time

The performance of the toehold exchange circuits is strongly dependent on the assembly time. To optimize the time of the reaction, the absorbance intensity of the biosensor in the presence of the target and non-complementary strands (as the negative control) for 3 hours was recorded. In Figure S3, the plot of absorbance versus time was represented for 0.3 nM of the target DNA. In this concentration, the largest signal to background ratio was obtained after a 1.5-hour incubation. However, I have reported the incubation time needed for the appearance of a detectable signal for 4 pM of the target DNA. Based on my experiments, the given signal was achieved after a 2-hour incubation. The detection limit of catalytic strand displacement–based assays (the strategy used in this study) heavily depends on the incubation time for interaction between the target and metastable DNA nanostructures [7]. Since in these methods, the depletion of the DNA nanostructures and the fuels halts the reaction, different initial concentrations of the target can consume all the substrates in different incubation times. Therefore, the plot of absorbance versus incubation time for lower concentrations of the target DNA reaches to plateau at longer incubation times.

3-4 Optimizing the toehold length

The behavior of toehold exchange circuits can be controlled by the length and the sequence of toehold domains (binding energy between toehold domain and its complementary counterpart) [15]. In this system, the properties of the target- and fuel-binding toeholds (domains 1* and 3* for the first layer and domains 5* and 7* for the second layer, respectively), especially toehold domains belonging to the first layer, determine the overall sensitivity and specificity of the circuit. In this respect, Song and coworkers conducted a study to find the optimum length and sequence of these toehold domains [23]. For a sequence with a 50% GC content, they found that the highest discrimination capability between perfect and spurious targets is achieved when the target- and fuel-binding toeholds are chosen with n and n-1 nucleotides, respectively. In the experimental conditions of the Song's system, the best value for n was determined to be 6 nucleotides. Since in the present system, the experimental conditions are different from the Song's system, we designed different target strands (T8/7, T7/6, and T6/5) that bind to 8, 7, and 6 nucleotides of the target-binding domain and leave 7 to 5 nucleotides as the fuel-binding domain on the S1 nanostructures, respectively (Figure S4). The target strands were separately added to the two-layer DNA circuit and the effect of toehold lengths on the circuit behavior was analyzed by releasing the hemin-binding aptamer in a colorimetric signaling readout. As shown in Figure 2, the highest signal to noise intensity is achieved with a target- and fuel-binding toehold containing 8 and 7 nucleotides, respectively.

It should be noted that the signal intensity of T9/8 (for other set of the substrate) was also obtained. The results showed that the signal intensity of T9/8 was slightly lower than the T8/7 (data not shown).

The results of a semi-empirical study conducted by Zhang and Winfree showed that in 1 M NaCl (or 11.5 mM $MgCl_2$) and 25 °C, toeholds longer than 7 nucleotides have no effect on the rate of toehold exchange reaction [15]. Based on different studies, deviation from 1 M NaCl and 25 °C to lower salt concentrations and higher temperatures can decrease the rate of DNA association and increase the rate of DNA dissociation reactions [24-26]. In the experimental conditions used in this study (0.22 M Na^+/K^+, 1.5 mM $MgCl_2$ and 37 °C), which were selected based on the optimum condition of the HRP-mimicking DNAzyme reaction [27-34], the DNA hybridization reaction proceeded in a way that the DNA melting reaction is favored over 1 M NaCl and 25 °C. To compensate for this issue, the selection of longer toeholds helps improve the behavior of the DNA circuit, especially via a decrease in the rate of DNA melting reaction.

3-5 Analyzing the sensitivity of the circuit

In order to find the sensitivity of the biosensor, we defined a limit of detection (LOD) for the two-layer DNA circuit in the optimum conditions (350 nM of the fuel strands and a 2-hour incubation time). The LOD of the biosensor was established based on the mean values plus three standard deviations of the negative controls (non-complementary strand). In this respect, absorbance

values greater than 0.085 were considered positive and values equal or lower than 0.085 were considered as negative. Different concentrations of the target strand (from 1 pM to 30 nM) were added to the circuit solution at the optimum conditions. The results showed that the two-layer circuit can detect target DNA with an LOD value equal to 4 pM (Figure 3). It should be noted that if the incubation time is increased to 3 hours, the biosensor can detect the target strand with an LOD value equal to 1 pM.

In order to evaluate the sensitivity of different layers of the biosensor, we implemented a one-layer DNA catalytic circuit containing the reagents belonging to the second layer of the biosensor. Different concentrations of the PI-2 strand, which acts as the input for the second layer, entered the circuit and the LOD of the second layer was solely measured. As shown in Figure 3, one-layer DNA circuit can detect DNA with an LOD value equal to 600 pM. Based on this analysis, it can be concluded that the two-layer DNA circuit can detect DNA 150 times more sensitive than the one-layer catalytic DNA circuit.

3-6 Analyzing the specificity of the circuit

In addition to the stability of toehold domain, the position of mismatch nucleotides from the toehold domain is another factor which can determine the capability of toehold exchange DNA circuits for mismatch discrimination [9]. To investigate the influence of mismatch position on discrimination capability, we designed three spurious targets where the mismatch nucleotides were located at the position 3, 6, and 9 of the displacement domain 2 of the target strand.

These positions were respectively referred to as the proximal (close to the toehold domain 1*), intermediate, and distal mismatches (Table S1). To evaluate the discrimination capability of the biosensor, we defined a discrimination factor (DF) based on (AbsT-AbsM)/(AbsT-AbsN), where AbsT, AbsM and AbsN are the absorbance intensities produced by the addition of complementary target (T), mismatched target (M), and the non-complementary strand (N), respectively (DF ranges from 0 to 1). The results showed that the proximal and intermediate mismatches have a similar DF close to 1 (0.98), while the distal mismatch has a DF of 0.85 (Figure 4). The discrepancy between the DF of proximal and distal mismatches can be interpreted by a change in the kinetic of DNA toehold exchange. Generally, any mismatch can provide an energy barrier for DNA toehold exchange reactions; however, a mismatch closer to the toehold domain presents a higher kinetic barrier than others [35, 36]. In this respect, it is suggested that the mismatched nucleotides of the target be located at the proximal or intermediate position when a circuit is designed.

3-7 Strategies to suppress the circuit leakage

In addition to these challenges, fuel-substrate leakage can decrease the signal to noise ratio in a toehold exchange circuit. In this type of circuit leakage, fuel strands react directly with the substrate nanostructures, yielding DNAzyme even in the absence of target strand. This is mostly due to base breathing near the end of helices, which provides a binding site for the fuel strands. To overcome this type of circuit leakage, we introduced G or C nucleotides at the

start and at the end of the fuel binding domains, that strongly suppress the blunt-end strand exchange reactions [10, 17]. The experimental results also confirmed this design rule so that the absorbance of negative control samples makes almost no changes during the reaction time.

3-8 Detection of target strand in serum samples

To evaluate the feasibility of the biosensor for detecting target DNA in a natural environment, several diluted serum samples were spiked with different concentrations of the target strand. The results of the target detection in the pure buffer were compared with a real biological sample. As shown in Figure 5, the absorbance intensities of the positive and the negative controls in serum samples were slightly higher than the pure buffer. Meanwhile, the LOD of the assay in this specimen was determined as low as 4 pM, which is similar to that found for the pure buffer. Recently, Zheng and co-workers have developed an enzyme-free signal amplification DNA circuit based on the catalytic hairpin assembly [21]. Their results showed that the signal intensity in saliva samples is significantly higher than the signal in a pure buffer for a given concentration. The authors have not provided any accounts of or justification for their results; but I surmise that the reason is related to the presence of proteins and other molecules, which act as crowding agents to increase the kinetic of the DNA strand displacement reaction. The increase in the rate of DNA strand displacement as a result of the presence of the molecular crowders has led to

more signals obtained over the same time course from a given concentration of the target DNA in serum samples.

Free DNA is known to be rapidly degraded by nucleases in serum, with a half-life varying from a few minutes to several hours. As a solution, I applied two strategies: 1) The serum samples were diluted in order to partially inhibit the nucleases [37], and 2) Serum samples were diluted in a solution containing "EDTA" [38]. Most single-strand-specific nucleases are either metalloenzymes or metal-requiring enzymes, and hence they are strongly inhibited by metal chelators like EDTA, EGTA, citrate and 8-hydroxyquinoline [39]. These two strategies guarantee the stability of single –stranded DNA in serum samples.

3-9 Generalizability of the signal amplification strategy

The signal amplification strategy presented in this study can be optimized for any nucleic acid with any length and sequence. It is well known that the trace amounts of circulating DNA and RNA are present in human blood [40]. The most potent target for present signal amplification system is microRNAs. A microRNA is a small non-coding RNA molecule (containing about 22 nucleotides single-stranded RNA) is found in plants, animals, and some viruses. In 2008, it was discovered that microRNAs are also present in human blood, where they were detected in plasma, platelets, erythrocytes, and nucleated blood cells [41]. The circulating microRNA increases in several diseases, including cancers [42], cardiovascular diseases [43], and microbial infections.

For longer DNA/RNA molecules or nucleic acids with specific secondary structures, however, the target must be, firstly, confined on the solid surface by, for instance, biotin-labeled oligonucleotides [1]. Then a second oligonucleotide, which contains a target-specific region and a universal translator [14], was added to the surface-confined target molecule. After hybridization of the target-specific region of the second oligonucleotide, the universal translator is overhung, and it can be used as a T8/7 target to produce a plenty of DNAzyme molecules.

Conclusion

In the present study, we developed a highly sensitive and specific bio-sensing platform on the basis of DNA catalytic circuit for the enzyme-free and colorimetric detection of nucleic acids. Four picomolars of the target DNA can be evaluated by naked eyes after only a 2-hour incubation with the circuit; meanwhile, if the incubation time is extended to 3 hours, the biosensor can detect 1 pM of the target DNA even in a complicated matrix such as serum samples. Since in the field of molecular diagnostics, enzyme-based amplifications tend to provide highly sensitive and specific detecting platforms, we compared the properties of these methods with the enzyme-free nucleic acid biosensors. As shown in Table 1, in comparison with the enzyme-free two-layer DNA circuit, the enzyme-based amplification systems provide an approximately 10-fold enhanced sensitivity and a slightly faster analysis time. However, the enzyme-free catalytic circuits provide a highly selective and cost-effective

platform for the detection of nucleic acids. It seems that the feature of molecular diagnosis can take advantage of enzyme-free DNA circuit to make clinical decisions more logically than today. In this respect, such studies help reveal the potential capabilities of enzyme-free DNA circuits for use in clinical diagnosis.

Acknowledgment

The authors acknowledge financial support for this investigation by the Research Council of Shahid Bahonar University (Kerman, Iran).

References

[1] H. Ravan, R. Yazdanparast, Development and evaluation of a loop-mediated isothermal amplification method in conjunction with an enzyme-linked immunosorbent assay for specific detection of Salmonella serogroup D, Anal. Chim. Acta, 733 (2012) 64-70.

[2] H. Ravan, R. Yazdanparast, Loop region-specific oligonucleotide probes for loop-mediated isothermal amplification–enzyme-linked immunosorbent assay truly minimize the instrument needed for detection process, Anal. Biochem., 439 (2013) 102-108.

[3] H. Ravan, R. Yazdanparast, Development of a new loop-mediated isothermal amplification assay for prt (rfbS) gene to improve the identification of Salmonella serogroup D, World J. Microbiol. Biotechnol., 28 (2012) 2101-2106.

[4] H. Ravan, S. Kashanian, N. Sanadgol, A. Badoei-Dalfard, Z. Karami, Strategies for optimizing DNA hybridization on surfaces, Anal. Biochem., 444 (2014) 41-46.

[5] X. Cao, Y. Ye, S. Liu, Gold nanoparticle-based signal amplification for biosensing, Anal. Biochem., 417 (2011) 1-16.

[6] T.N. Grossmann, O. Seitz, Nucleic acid templated reactions: consequences of probe reactivity and readout strategy for amplified signaling and sequence selectivity, Chem. Asian J., 15 (2009) 6723-6730.

[7] G. Seelig, D. Soloveichik, D.Y. Zhang, E. Winfree, Enzyme-free nucleic acid logic circuits, Science, 314 (2006) 1585-1588.

[8] D.Y. Zhang, A.J. Turberfield, B. Yurke, E. Winfree, Engineering entropy-driven reactions and networks catalyzed by DNA, Science, 318 (2007) 1121-1125.

[9] D.Y. Zhang, S.X. Chen, P. Yin, Optimizing the specificity of nucleic acid hybridization, Nat. Chem., 4 (2012) 208-214.

[10] D.Y. Zhang, E. Winfree, Robustness and modularity properties of a non-covalent DNA catalytic reaction, Nucleic Acids Res., 38 (2010) 4182-4197.

[11] Y.-J. Chen, N. Dalchau, N. Srinivas, A. Phillips, L. Cardelli, D. Soloveichik, G. Seelig, Programmable chemical controllers made from DNA, Nat. Nanotech., 8 (2013) 755-762.

[12] M. Cook, D. Soloveichik, E. Winfree, J. Bruck, Programmability of chemical reaction networks, Algorithmic Bioprocesses, Springer 2009, pp. 543-584.

[13] C. Jung, A.D. Ellington, Diagnostic applications of nucleic acid circuits, Acc. Chem. Res., 47 (2014) 1825-1835.

[14] H. Ravan, Translating nucleic-acid hybridization into universal DNA-reporter sequences, Trends Anal. Chem., 65 (2015) 97-106.

[15] D.Y. Zhang, E. Winfree, Control of DNA strand displacement kinetics using toehold exchange, J. Am. Chem. Soc., 131 (2009) 17303-17314.

[16] B. Yurke, A.J. Turberfield, A.P. Mills, F.C. Simmel, J.L. Neumann, A DNA-fuelled molecular machine made of DNA, Nat., 406 (2000) 605-608.

[17] L. Qian, E. Winfree, Scaling up digital circuit computation with DNA strand displacement cascades, Science, 332 (2011) 1196-1201.

[18] Y. Wang, J. Wang, F. Yang, X. Yang, Spectrophotometric detection of lead (II) ion using unimolecular peroxidase-like deoxyribozyme, Microchim. Acta, 171 (2010) 195-201.

[19] T. Li, S. Dong, E. Wang, G-Quadruplex aptamers with peroxidase-like DNAzyme functions: which is the best and how does it work? Chem. Asian J., 4 (2009) 918-922.

[20] Y. Zhao, L. Zhou, Z. Tang, Cleavage-based signal amplification of RNA, Nat. Commun., 4 (2013) 1493.

[21] A.-X. Zheng, J. Li, J.-R. Wang, X.-R. Song, G.-N. Chen, H.-H. Yang, Enzyme-free signal amplification in the DNAzyme sensor via target-catalyzed hairpin assembly, Chem. Commun., 48 (2012) 3112-3114.

[22] D.Y. Zhang, Towards domain-based sequence design for DNA strand displacement reactions, DNA Computing and Molecular Programming, Springer 2011, pp. 162-175.

[23] T. Song, S. Xiao, D. Yao, F. Huang, M. Hu, H. Liang, An Efficient DNA-Fueled Molecular Machine for the Discrimination of Single-Base Changes, Adv. Mater. 26 (2014) 6181-6185.

[24] I.I. Cisse, H. Kim, T. Ha, A rule of seven in Watson-Crick base-pairing of mismatched sequences, Nat. Struct. Mol. Biol., 19 (2012) 623-627.

[25] T.E. Ouldridge, P. Šulc, F. Romano, J.P. Doye, A.A. Louis, DNA hybridization kinetics: zippering, internal displacement and sequence dependence, Nucleic Acids Res., 41 (2013) 8886-8895.

[26] N. Srinivas, T.E. Ouldridge, P. Šulc, J.M. Schaeffer, B. Yurke, A.A. Louis, J.P. Doye, E. Winfree, On the biophysics and kinetics of toehold-mediated DNA strand displacement, Nucleic Acids Res., 41 (2013) 10641-10658.

[27] P. Travascio, Y. Li, D. Sen, DNA-enhanced peroxidase activity of a DNA aptamer-hemin complex, Chemistry & biology, 5 (1998) 505-517.

[28] Y. Guo, L. Zhou, L. Xu, X. Zhou, J. Hu, R. Pei, Multiple types of logic gates based on a single G-quadruplex DNA strand, Sci. Rep., 4 (2014).

[29] Y. Guo, J. Cheng, J. Wang, X. Zhou, J. Hu, R. Pei, Label-Free Logic Modules and Two-Layer Cascade Based on Stem-Loop Probes Containing a G-Quadruplex Domain, Chem. Asian J., 9 (2014) 2397-2401.

[30] Y. Guo, Q. Wang, Z. Wang, X. Chen, L. Xu, J. Hu, R. Pei, Label-free detection of T4 DNA ligase and polynucleotide kinase activity based on toehold-

mediated strand displacement and split G-quadruplex probes, Sens. Actuator B-Chem., 214 (2015) 50-55.

[31] Y. Seok, J.-Y. Byun, H. Mun, M.-G. Kim, Colorimetric detection of PCR products of DNA from pathogenic bacterial targets based on a simultaneously amplified DNAzyme, Microchem. Acta, 181 (2014) 1965-1971.

[32] J. Nie, D.-W. Zhang, F.-T. Zhang, F. Yuan, Y.-L. Zhou, X.-X. Zhang, Reporter-triggered isothermal exponential amplification strategy in ultrasensitive homogeneous label-free electrochemical nucleic acid biosensing, Chem. Commun., 50 (2014) 6211-6213.

[33] Z. Cheglakov, Y. Weizmann, B. Basnar, I. Willner, diagnosing viruses by the rolling circle amplified synthesis of DNAzymes, Org. Biomol. Chem., 5 (2007) 223-225.

[34] J. Dong, X. Cui, Y. Deng, Z. Tang, Amplified detection of nucleic acid by G-quadruplex based hybridization chain reaction, Biosens. Bioelectron., 38 (2012) 258-263.

[35] R.R. Machinek, T.E. Ouldridge, N.E. Haley, J. Bath, A.J. Turberfield, Programmable energy landscapes for kinetic control of DNA strand displacement, Nat. Communi., 5 (2014).

[36] J.S. Wang, D.Y. Zhang, Simulation-guided DNA probe design for consistently ultraspecific hybridization, Nat. Chem., 7 (2015) 545-553.

460 [37] W. Prince, D. Baker, A. Dodge, A. Ahmed, R. Chestnut, D. Sinicropi,
461 Pharmacodynamics of recombinant human DNase I in serum, Clin. Exp.
462 Immunol., 113 (1998) 289.

463 [38] G.B. Barra, T.H. Santa Rita, J. de Almeida Vasques, C.F. Chianca, L.F.A.
464 Nery, S.S.S. Costa, EDTA-mediated inhibition of DNases protects circulating
465 cell-free DNA from ex vivo degradation in blood samples, Clin. Biochem., 48
466 (2015) 976-981.

467 [39] N.A. Desai, V. Shankar, Single-strand-specific nucleases, FEMS Microbiol.
468 Rev., 26 (2003) 457-491.

469 [40] B.V. Vu, K.L. Anthony, U. Strych, R.C. Willson, Recovery of Small DNA
470 Fragments from Serum Using Compaction Precipitation, PLoS One, 7 (2012)
471 e51863.

472 [41] E.E. Creemers, A.J. Tijsen, Y.M. Pinto, Circulating microRNAs novel
473 biomarkers and extracellular communicators in cardiovascular disease? Circ.
474 Res., 110 (2012) 483-495.

475 [42] H. Schwarzenbach, N. Nishida, G.A. Calin, K. Pantel, Clinical relevance of
476 circulating cell-free microRNAs in cancer, Nat. Rev. Clin. Oncol., 11 (2014) 145-
477 156.

478 [43] F. Wang, C. Chen, D. Wang, Circulating microRNAs in cardiovascular
479 diseases: from biomarkers to therapeutic targets, Front Med., 8 (2014) 404-
480 418.

481

Figure legends

Figure 1- Schematic illustration of the two-layer feed-forward catalytic DNA circuit. Each DNA sequence contains several functional domains labeled numerically. Upon binding of the target strand to the DNA nanostructure S1, the circuit is run in order that at the end a hemin-binding aptamer, with the ability to convert a colorless substrate into a colored substance, is released.

Figure 2- Effects of different target strands with different toehold lengths on the signal intensity of detection system. The bars represent the intensity of absorbance at 414 nm with different target strands (T8/7, T7/6, and T6/5) (0.3 nM) and negative control.

Figure 3- Comparison between the detection sensitivity of the two-layer feed-forward catalytic DNA circuit (Two-layer in graph) and the second layer of the circuit (One-layer in graph). Cut-off value represents the limit of detection for the circuits.

Figure 4- Signal intensity of two-layer catalytic DNA circuit at 414 nm in the presence of 0.3 nM target strand (T), 10 nM non-complementary strand (Negative) 10 nM proximal mismatched target (Proximal), 10 nM intermediate mismatched target (Intermediate), and 10 nM distal mismatched target (Distal).

Figure 5- Target DNA detected by two-layer catalytic DNA circuit in buffer and in 1:6 dilution of serum samples. The graphs represent the difference in absorbance intensity of the target DNA and the cut-off value in the pure buffer

503 and serum samples. The concentration of S1 and S2 was 300 nM and the
504 concentration of the fuel strands was 350 nM.

505 **Supplementary Figure Legends**

506 **Figure S1-** Non-denaturing PAGE (12%): from left to right; lane 1- 10 bp DNA
507 Ladder, lane 2- S1 nanostructure, lane 3- S2 nanostructure, lane 4- 300 nM
508 S1+ 300 nM S2+ 350 nM of each fuel strands (after a two-hour incubation),
509 lane 4- 300 nM S1+ 300 nM S2+ 350 nM of each fuel strands + 0.3 nM of the
510 Target strand T (after a two-hour incubation).

511 **Figure S2-** Effect of the fuels concentration on the signal intensity of the
512 detection system. The graph represents the intensity of absorbance at 414 nm
513 with target strand (0.3 nM). The concentration of S1 and S2 was 300 nM. The
514 concentration of the fuel strands varied from 300 nM to 360 nM.

515 **Figure S3-** Effect of the assembly time on the signal intensity of the detection
516 system. The bars represent the intensity of absorbance at 414 nm with (0.3
517 nM) or without the target strand. The concentration of S1 and S2 was 300 nM
518 and the concentration of the fuel strands was 350 nM.

519 **Figure S4-** The position of different target strands (T8/7, T7/6, and T6/5) on
520 the S1 nanostructure.

521

522

Table 1- Comparison of different enzyme-based and enzyme-free bio-sensing strategies for detection of nucleic acids.

System	Detecting strategy	Assay time (h)	Detecting indicator	LOD (M)	Ref.
PCR*-HRP mimicking DNAzyme	Enzyme-based	2	Colorimetric	1×10^{-10}	[31]
EXPAR**-HRP mimicking DNAzyme	Enzyme-based	1	Colorimetric	2.5×10^{-12}	[32]
RCA***-HRP mimicking DNAzyme	Enzyme-based	2	Colorimetric	1×10^{-13}	[33]
HCR-HRP mimicking DNAzyme	Enzyme-free	2	Colorimetric	7.5×10^{-9}	[34]
CHA-HRP mimicking DNAzyme	Enzyme-free	2	Colorimetric	2×10^{-11}	[21]
Two-layer catalytic circuit	Enzyme-free	2	Colorimetric	4×10^{-12}	Present study

* PCR: Polymerase Chain Reaction
**EXPAR: isothermal EXPonential Amplification Reaction
***RCA: Rolling Circle Amplification

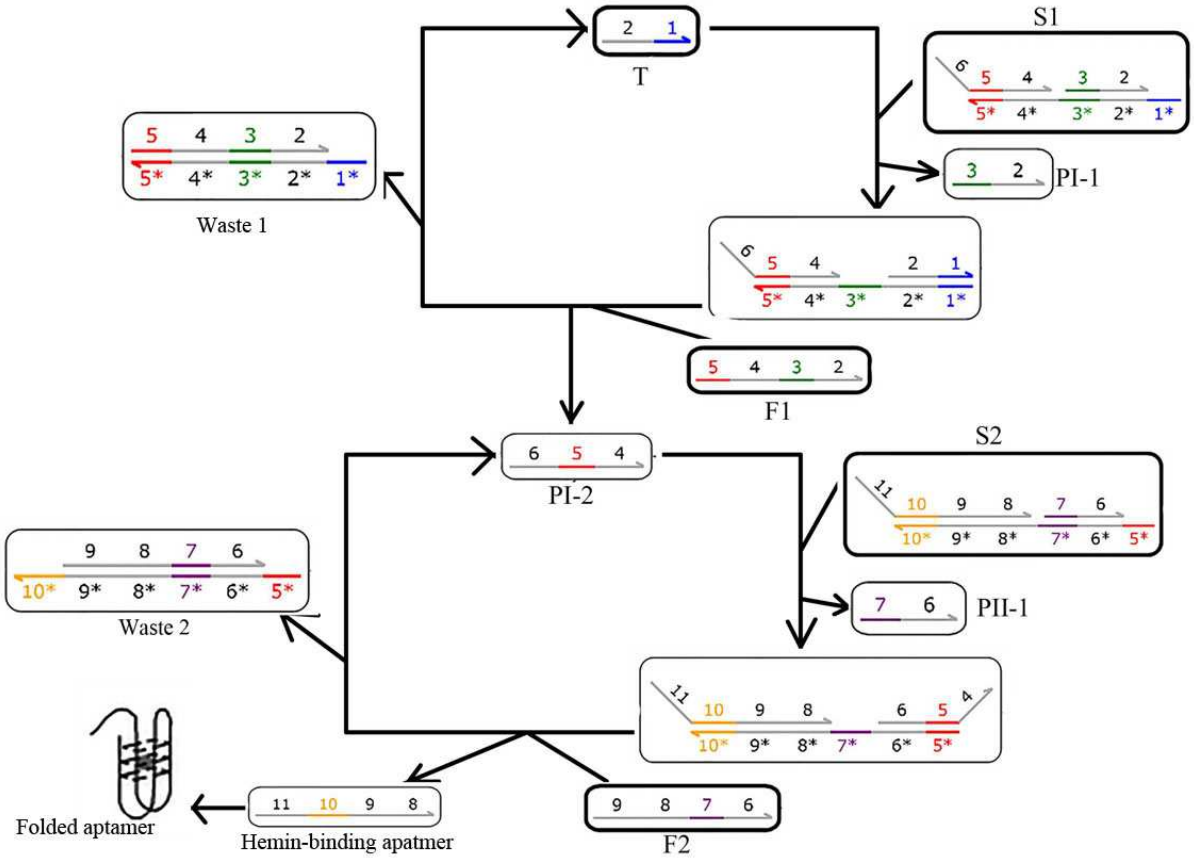

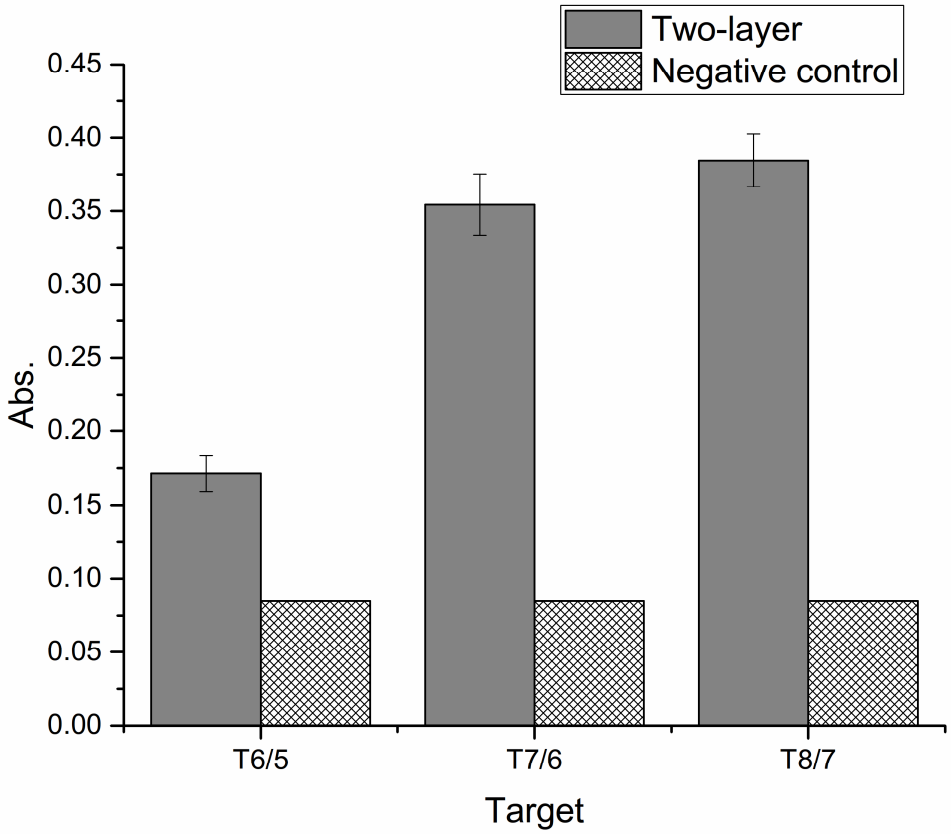

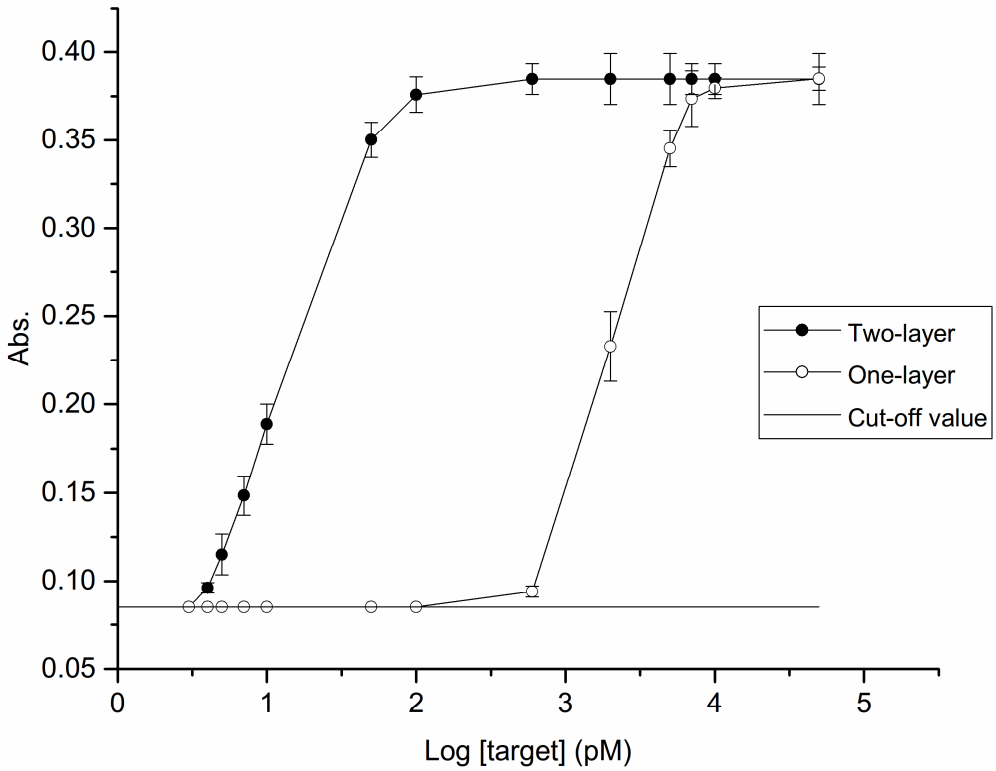

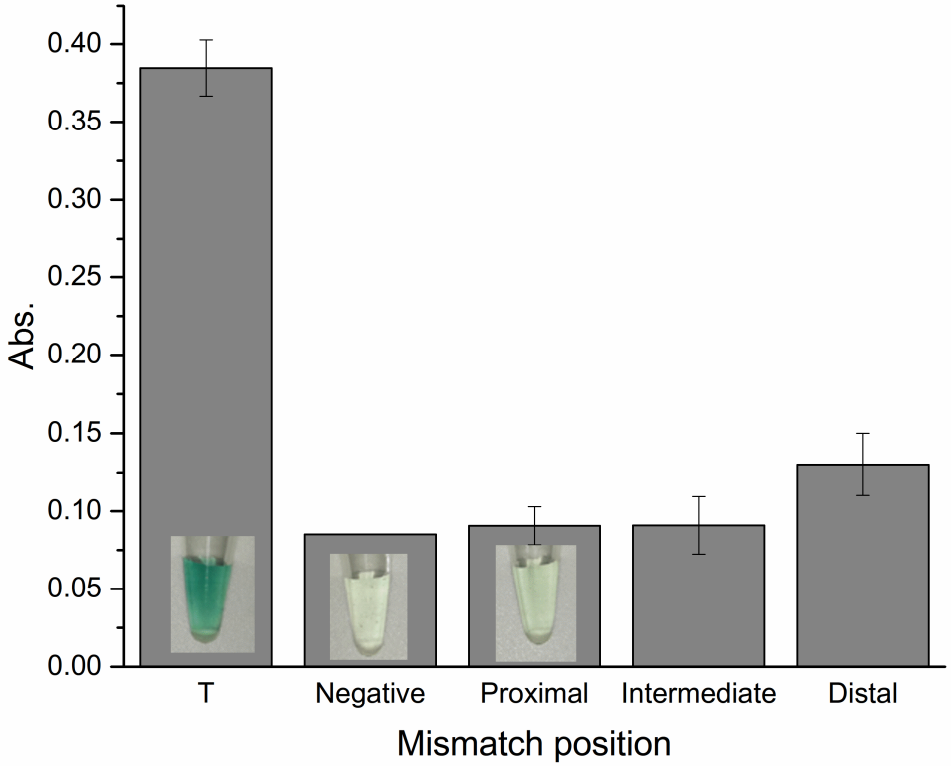

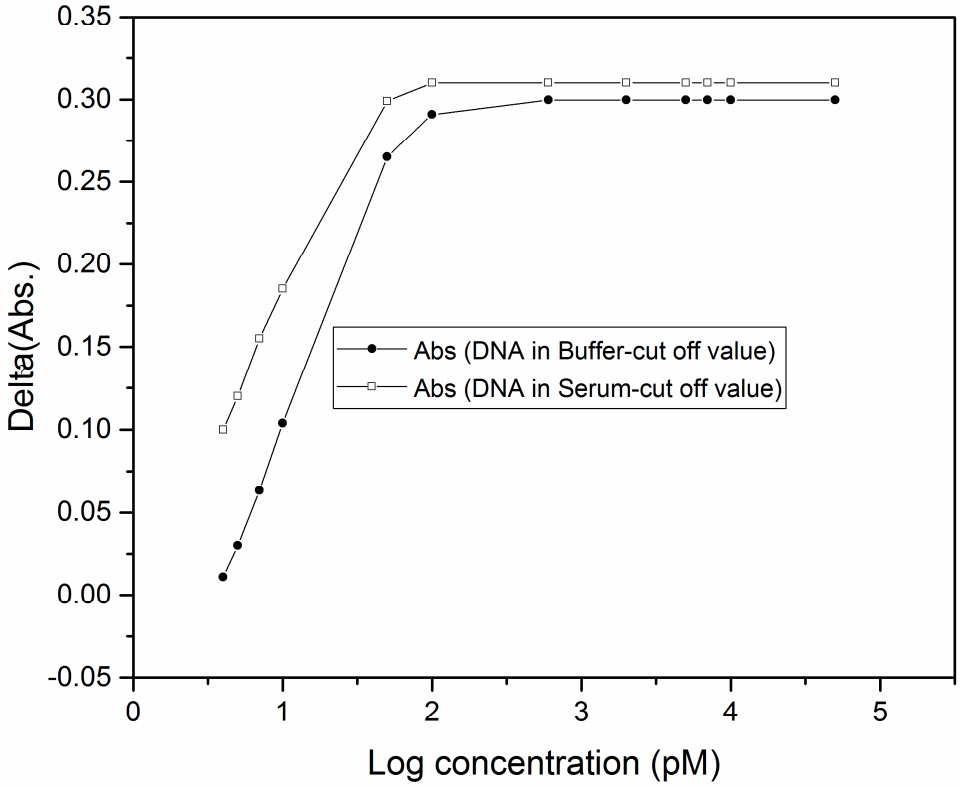

Highlights

- A catalytic DNA circuit for enzyme-free and colorimetric detection of nucleic acids
- The circuit can detect 4 pM of the target DNA after a 2-hour incubation
- The circuit can truly discriminate a spurious target with one nucleotide mismatch